Lecture Notes in Earth Sciences

Edited by Somdev Bhattacharji, Gerald M. Friedman,
Horst J. Neugebauer and Adolf Seilacher

29

Fritz K. Brunner Chris Rizos (Eds.)

Developments in Four-Dimensional Geodesy

Selected papers of the
Ron S. Mather Symposium on Four-Dimensional Geodesy
Sydney, Australia, March 28–31, 1989

Springer-Verlag
Berlin Heidelberg New York London Paris Tokyo Hong Kong

Lambeck, K., 1990. Glacial rebound and sea-level change: an example of deformation of the Earth by surface loading.
In: Developments in Four-Dimensional Geodesy, (F.K. Brunner and C. Rizos, Eds), Springer-Verlag, 111-137.

Glacial Rebound and Sea-Level Change: An example of Deformation of the Earth by Surface Loading

K. Lambeck
Australian National University
Australia

ABSTRACT:

One of the more important illustrations of the earth's response to external forcing is provided by the glacial rebound problem. The melting of the Late Pleistocene ice sheets and the distribution of meltwater into the oceans provides a time dependent and spatially variable surface load. A principal observation of the response of the earth to this change is in the relative shift in position of sea-level and the crust. Observations of this response provide constraints on the mantle rheology as well as on the glacial unloading process. This paper sketches out the problem, develops the sea-level equation and its solution and discusses the convergence requirements of the latter. It then discusses the principal characteristics of the global sea-level change and illustrates how earth and ice parameters can be separated by examining sea-level data in different areas, at different time intervals, and by using differential techniques. The final section summarizes some of the principal results and unresolved questions.

1. INTRODUCTION

Geomorphological observations have revealed a complex pattern of sea-level change for the past 18 000 years that are associated with the last deglaciation of the Late Pleistocene ice sheets. Near the centres of former glaciation the sea-level has dropped relative to the crust by hundreds of metres, while far from these centres, sea-level has risen by typically 130-150m. These observations are important for studying the tectonic histories of continental margins and ocean islands, for evaluating the mechanical response of the Earth to surface loading on time scales of 10^3-10^4 years, for constraining the melting histories of the large polar ice sheets, and for understanding present sea-level change.

The recognition that raised and warped shorelines in northern Europe reflected the Earth's response to glacial unloading go back to the nineteenth century and early attempts to quantify this response were made by Daly, Haskell, Niskanen, Vening Meinesz and others. The plate tectonics hypothesis, with the need to establish estimates of the mantle viscosity, resulted in a renewed interest in the problem and major contributions were made by McConnell (1968), Walcott (1972), Cathles (1975), Farrell and Clark (1976), and Peltier and Andrews (1976). Yet today, the problem is still not solved and continues to attract attention, in part because of the renewed interest in present and future sea-level change as a possible result of the enhanced Greenhouse effect. One reason for the lack of solution in the many faceted nature of the problem. Other than developing modelling procedures, models for the waxing and waning of the ice sheets need to be improved. The base of observational evidence for relative sea-level change also needs to be carefully evaluated and expanded upon.

The emphasis of this paper is on the geophysical modelling of the sea-level change produced by the melting of the ice sheets. Recent work has shown that in order to obtain realistic predictions a very high spatial resolution of the sea-level is required, whether this be at positions near the ice sheet or far from any centre of glaciation. Once achieved, these solutions begin to explain the complex patterns of change observed in a variety of regions; along the Australian shoreline, between nearby Pacific islands, or in northwestern Europe.

2. THE GLACIAL REBOUND PROBLEM

Consider a rigid planet partially covered by ocean. The sea surface will be an equipotential whose shape is determined by the gravity field of the planet and of the ocean waters. Extraction of water from the ocean to form an ice sheet leads to an overall lowering of the sea-level but not by a uniform amount because the redistribution of mass on the rigid planet's surface changes the shape of the equipotential surfaces.

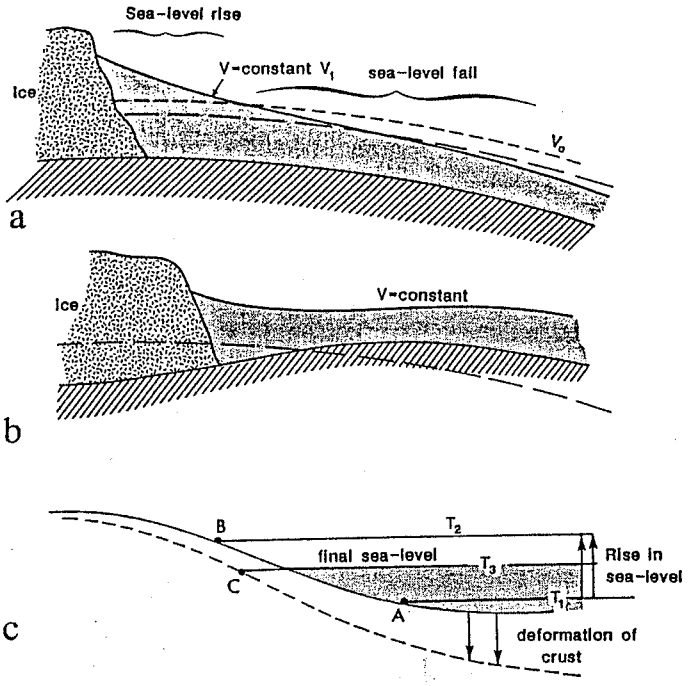

Figure 1: Schematic illustration of the shape of the sea surface in response to glaciation.

(a) Near the edge of an ice sheet on a rigid planet. When the ice sheet forms water is extracted from the ocean reducing the equivalent sea-level, but because of the gravitational attraction of the ice and water the sea-level change is not uniform.

(b) Same as (a) but for a deformable Earth.

(c) Far from the ice sheet along a continental margin. At time T_1 the sea level begins to rise rapidly up to the time T_2 and the shore line moves from point A to B. In this interval and afterwards the crust responds to this loading by subsiding beneath the oceans and rising beneath the continent, producing a tilting of the margin. Thus at time $T_3 > T_2$ sea-level actually appears to drop (point C).

Near the newly formed ice sheet the equipotential surface is pulled up and, depending on the new mass distribution, sea-level may actually be higher than before. As melting occurs sea-level drops in the vicinity of the ice sheet in response to the modification of the equipotential surface and at the same time it rises as the volume of the ocean increases (Figure 1a). On a deformable planet the growing ice sheet loads the crust and induces flow in the mantle away from the loaded area while the reduced water load produces a rebound of the oceanic crust. The shape of the sea-surface is now determined by the time dependent gravity field of the solid body as well as that of the ice and water load (Figure 1b). Within and near the ice sheets, the response of the crust is primarily determined by the change in the ice load. Further away, where typically

the fluctuations in sea-level are about 100 m, the crustal adjustments to the changing water load are of the order of 30 m.

Consider sea-level at a continental margin, far from the ice sheets. As meltwater is added into the oceans the sea floor is loaded and the sub-ocean mantle is stressed and mantle flow occurs from beneath the continent. The amount of deformation will be a function of the magnitude and spatial distribution of the water load, of the flow properties of the mantle, and of the mechanical properties of the lithosphere, but generally there will be a tilting of the margin (Figure 1c). At ocean islands the additional meltwater loads the sea floor uniformly about the island and the sea floor is depressed taking the island with it. But if the island is large, sub-lithospheric flow occurs from beneath the ocean to beneath the island and the later will tend to rise, resulting in a differential response between the island and the sea-floor.

What emerges from this heuristic description is a sea-level that displays complex spatial and temporal patterns of change. A zero order approximation of this change is provided by the time-dependent equivalent sea-level (esl), defined as

$$\zeta_{esl} = \zeta_o = \text{(change in ocean volume)/(ocean surface area)} \quad (1)$$

Spatial departures from this can be large and this definition has limited usefulness beyond being an estimate of the change in ocean volume. A more appropriate definition of the sea-level is

$$\zeta = \zeta_r + \zeta_i + \zeta_w \quad (2)$$

where ζ_r is the sea-level change that would occur on a rigid Earth, and includes ζ_{esl}. The second term ζ_i is the additional change produced by the response of the crust to the changing ice volume and ζ_w is the further adjustment produced by the response of the crust to the changing water load.

The relative importance of the three terms varies with time and position. It is therefore useful to discuss sea-level during the Late Pleistocene-Early Holocene, from about 20,000 to 8,000 years ago when ice melting occurred, and during the post-melting period of 8,000 years to the present. It is also useful to discuss sea-level for different regions: the far-field, the region far from the ice sheet where the primary contributions are ζ_{esl} and ζ_w; the near-field, being the region near the margin of the ice sheet where the dominant contribution comes from ζ_r and ζ_i ; the intermediate field between these two regions; and the region within the ice sheet margin where the dominant form is ζ_i. Characteristic sea-level curves can be established for each area (Figure 2) but considerable variation occurs within each zone and no simple zoning occurs.

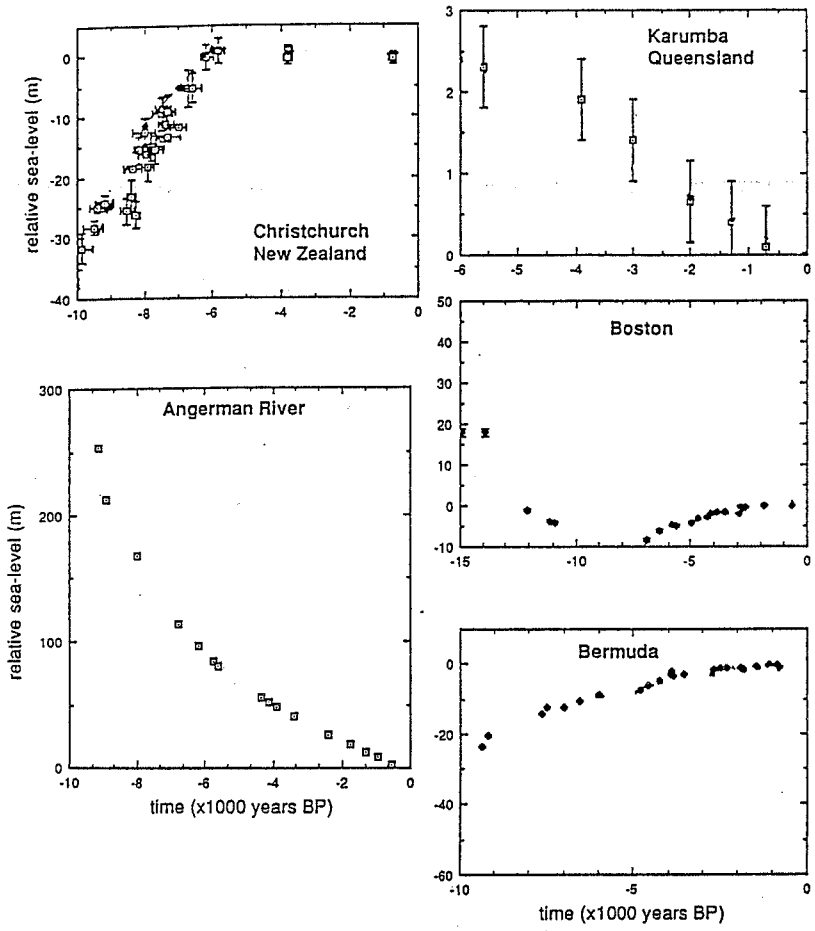

Figure 2: Characteristic sea-level observations

(a) far-field in late Pleistocene and Holocene time (Christchurch, New Zealand)
(b) far-field in late Holocene time (Karumba, Gulf of Carpenteria, Queensland)
(c) near-field (Boston, Massachusetts)
(d) intermediate-field (Bermuda)
(e) site near centre of former Fennoscandian ice sheet (Angerman River, Gulf of Bothnia).

3. THE SEA LEVEL EQUATION

The sea-level variation can be defined by using a Green's function formulation for the change in gravitational potential due to the redistribution of the surface load. For a rigid Earth, the potential at a point $\mathbf{r}$ due to the ice load $\mathbf{r}'$ is given by

$$V_i(\mathbf{r}) = \int_{A_i} \mathcal{G}_V(|\mathbf{r}-\mathbf{r}'|)\, \rho_i\, \zeta_i(\mathbf{r}')\, dA \tag{3}$$

where ζ_i is the ice height at $\mathbf{r}'$, ρ_i is the ice density, $\mathcal{G}_V$ in the potential Green function

$$\mathcal{G}_V = \frac{G}{R} \sum_{n=0}^{\infty} P_n(\cos\psi) \tag{4}$$

where P_n are Legendre polynomials and ψ is the angular separation of $\mathbf{r}$ and $\mathbf{r}'$. The integral is over the surface area of the ice. The radial shift in the equipotential surface due to the ice load is V_i/g or $(3\rho_i/4\overline{\rho})\ \Sigma_n I_n$ where

$$I_n = R^{-2} \int_{A_i} \zeta_i(\mathbf{r}')\ P_n(\cos\psi)\, dA \tag{5}$$

and $\overline{\rho}$ is the mean density of the Earth. The change in sea-level caused by this potential alone is

$$\zeta' = \{V_i - \langle V_i \rangle_o\}/g \tag{6}$$

where $\langle\ \rangle_o$ denotes the average value taken over the ocean. This is

$$\zeta' = -\frac{3}{4\pi}\ \frac{\rho_i}{\rho_o}\ \sum_n (I_n - \langle I_n \rangle_o)\ . \tag{7}$$

To this must be added the meltwater flowing into the ocean

$$\zeta'' = \{\zeta_o + V_w - \langle V_w \rangle_o\}/g \tag{8}$$

where ζ_o is the equivalent sea-level (c.f. eqn 1)

$$\zeta_o = -M_i / 4\pi R^2\, o_{100}\, \rho_w \tag{9}$$

where M_i is the change in total ice mass, considered to be positive for a growing ice sheet. $o_{100} \simeq 0.70$ is the zero degree term in the ocean function expansion. V_W is the potential of the water load, or analogous to (3),

$$V_w(\mathbf{r}) = \int_{A_o} \mathcal{G}_V(|\mathbf{r}-\mathbf{r}'|)\, \rho_w\, \zeta(\mathbf{r}')\, dA \tag{10}$$

where ζ is the sea-level change and the integral is over the ocean area A_o. Then the final change in sea-level is, still for the rigid Earth model,

$$\zeta = \zeta_r = \zeta_o - \frac{3}{4\pi}\frac{\rho_i}{\rho_o}\sum_n (I_n - \langle I_n \rangle_o) + \frac{3}{4\pi}\frac{\rho_w}{\rho}\sum_n (J_n - \langle J_n \rangle_o) \qquad (11)$$

with

$$J_n = R^{-2} \int_{A_o} \zeta(r')\, P_n(\cos\psi)\, dA \quad . \qquad (12)$$

This equation defines the change in sea-level with time and position on a rigid Earth due to the melting of ice and the addition of this meltwater into the ocean. The sea-level change ζ enters on both sides, on the right hand side through the integral J_n, and the equation is an integral equation that is solved by an iterative procedure. Mass is conserved and the sea-level remains an equipotential surface throughout.

For an elastic planet the Green's functions become

$$\mathcal{G}_V = \frac{G}{R}\sum_{n=0}^{\infty} (1 + k_n' - h_n')\, \rho_n(\cos\psi) \qquad (13)$$

where k_n', h_n' are the load Love numbers. The sea-level change on the elastic planet now is (c.f. eqn 2)

$$\zeta_e = \zeta_r + \delta\zeta_e \qquad (14)$$

where the elastic contribution is

$$\delta\zeta_e = -\frac{3}{4\pi\bar{\rho}}\left[\rho_i \sum_n (I_n' - \langle I_n' \rangle_o)\, r - \rho_w \sum_n (J_n' - \langle J_n' \rangle_o)\right] \qquad (15)$$

with

$$I_n' = R^{-2} \int_{A_i} \zeta_i(r')\, (k_n' - h_n')\, P_n(\cos\psi)\, dA \qquad (16)$$

and a similar definition for J_n'. On a viscoelastic planet

$$\zeta_{ve} = \zeta_r + \delta\zeta_{ve} \qquad (17)$$

where, by using the correspondence principle (e.g. Peltier 1974),

$$\delta\zeta_{ve}(\varphi,\lambda;t) = \mathcal{L}^{-1}\{\delta\zeta_e(\varphi,\lambda:s) \qquad (18)$$

and where $\mathcal{L}$ is the Laplace transform, $\mathcal{L}^{-1}$ is the inverse transform, and s is the Laplace transform parameter of dimension time^{-1}. Then $\delta\zeta_e(s)$ is of the same form as (15,16) but in which the I_n' and J_n' are replaced by their transforms, for example,

$$I_n' \Rightarrow \hat{I}_n' = R^{-2} \int_{A_i} \hat{\zeta}_i(\hat{k}_n' - \hat{h}_n') P_n(\cos\psi)\, dA \qquad (19)$$

where $\hat{k}_n'$, $\hat{h}_n'$ are the load Love numbers in the Laplace transform domain. The resulting sea-level equation can now be written as (c.f. equation 2)

$$\zeta = \zeta_r + \zeta_i + \zeta_w \qquad (20)$$

where

$$\zeta_i = Z_1 - \langle Z_1 \rangle \quad , \quad \zeta_w = Z_2 - \langle Z_2 \rangle \qquad (21)$$

with

$$Z_1 - \frac{3\rho_i}{4\pi\bar{\rho}} \int_{A_i} \mathcal{L}^{-1}\left[(\hat{k}_n - \hat{h}_n)\,\hat{\zeta}_i(s)\right] P_n(\cos\psi)\, dA_i) \qquad (22)$$

and

$$Z_2 - \frac{3\rho_w}{4\pi\bar{\rho}} \sum_n \int_{A_o} \left[\int_{A_i} \mathcal{L}^{-1}\left[(\hat{k}_n - \hat{h}_n)\,\hat{\zeta}_i(s)\right] dA_i \right] P_n(\cos\psi)\, dA_o \qquad (23)$$

where the summation over n is from 0 to ∞, at least in principle. This sea-level equation is essentially that of Farrell and Clark (1976), and has been used by Peltier and Andrews (1976), Wu and Peltier (1983), Nakiboglu et al. (1983), and Nakada and Lambeck (1987).

Solutions of the sea-level equation require a knowledge of the evolution of the ice loads $\zeta_i(\varphi,\lambda{:}t)$ through space and time and of the viscosity structure of the planet through the Love numbers $(\hat{k}_n' - \hat{h}_n')$. Expressions for the latter can be derived for simple Earth models (e.g. Lambeck, 1988, p. 67) but for realistic solutions complete Earth models are essential. The elastic parameters and density are given by the seismic models but the viscosity is largely unknown and to be determined from the observations. Figure 3 illustrates these Love numbers in the Laplace transform domain for the elastic Earth model of Dziewonski and Anderson (1981), a constant mantle viscosity of 10^{21} Pas s, and a high viscosity (10^{25} Pa s) lithosphere of 50 km thickness. For large s, corresponding to small t, the response approaches that of an elastic planet.

For small s ($s \lesssim 10^{-4}$ a^{-1}) the response approaches that of an elastic shell over a fluid mantle in which all load stresses have relaxed. Further evolution of the response occurs with smaller s as stresses relax in the lithosphere. These results can therefore be interpreted qualitatively as a relaxation spectra for harmonic loads. Figure 4 illustrates the corresponding time dependent Love numbers $\mathcal{L}^{-1}$ ($\hat{k}_n'$ - $\hat{h}_n'$) for a step function surface load. At time t = 0, the response is that of an elastic body and with time the response decays to a limit corresponding, in this case, to the elastic response of a 50 km thick elastic shell overlying a fluid interior. By t = 20,000 years, much of the load-induced stresses have relaxed within the viscoelastic mantle.

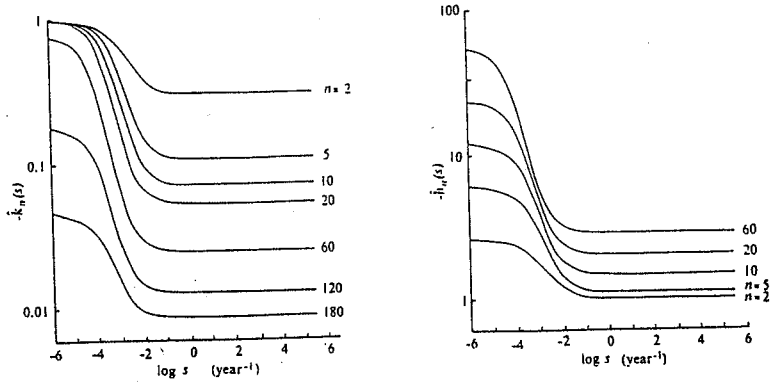

Figure 3: Load Love numbers $\hat{h}_n(s)$, $\hat{k}_n(s)$ as a function of the Laplace transform variable s (years^{-1}).

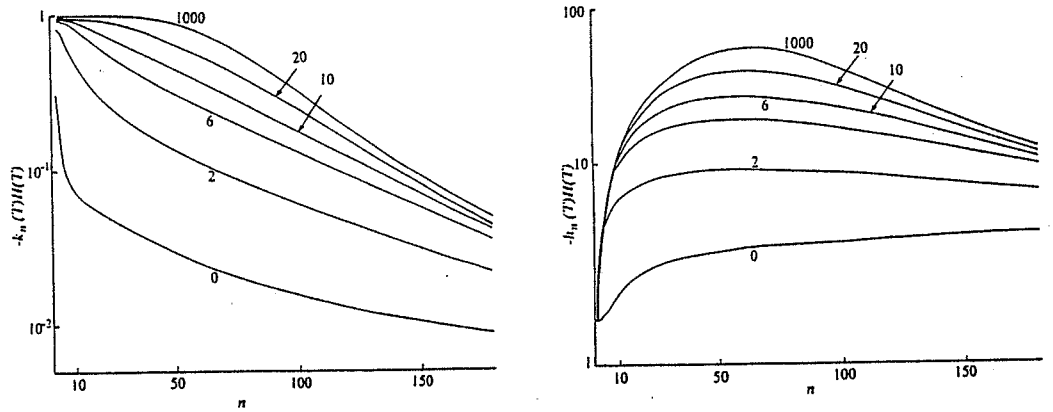

Figure 4: Load Love numbers k, h as a function of time (in units of 1000 years).

It has been shown by Peltier (1974) that the $(\hat{k}_n' - \hat{h}_n')$ can be adequately expanded numerically into the form

$$(\hat{k}_n' - \hat{h}_n') = \sum_{i=1}^{m} \frac{C_n^i}{S+S_i} + \left[k_e^n - h_e^n\right] \qquad (24)$$

where k_e^n , h_e^n are elastic load Love numbers. This is essentially an eigen function expansion in which the S_i correspond to the eigen values. This expansion is also used here in reaching solutions of equations (20)-(23).

The solution of the sea-level equation also requires a model of the temporal and spatial distribution of the ice load. The observed quantities are the limits of the ice sheet as the last glaciers receded and this is complemented with mechanical models for the ice sheets (e.g. Paterson, 1972; Hughes 1981). A critical unknown in this calculation is the amount of isostatic compensation that has occurred beneath the load. The effect of the delay in the isostatic response is another vexing question and it means that the ice models are not free from assumptions about the Earth's response to loading. Another major assumption in these reconstructions is whether the ice sheets are in static equilibrium or whether dynamic non-equilibrium models are more appropriate in which the ice volumes are driven by external climatic forcing and feedback mechanisms (Budd and Smith, 1981, 1987). The direct observations of the isochrones are usually restricted to the last 20,000 years and the earlier record is less clear, often inferred indirectly from palaeoclimatic or isotopic signatures or from the variations in sea-level itself (e.g. Chappell and Shackleton, 1986).

In the present formulation the ice sheets are described by ice columns of defined areal extent and whose height varies linearly with time in the interval t_j and t_{j+1} so that for column m and time t

$$\zeta_{mj}(t) = a_j t + b_j \qquad t_j \le t \le t_{j+1} \qquad (25)$$

The entire melting history is defined by a total of m such columns over r time intervals. The corresponding Laplace transforms are then convolved with the numerical transforms (24) of the Earth's response in order to evaluate the integrals Z_1, Z_2 (equations 22, 23) and the sea-level change (equation 20). Details are given in Nakada and Lambeck (1987).

4. CONVERGENCE REQUIREMENTS

If high resolution solutions of the sea-level equation are sought then the geometry of the surface loads must be known with very considerable detail. From eqns (20)-(23) the change in the sea-level with respect to the present day value $\zeta(t_o)$ can be written as

$$\Delta\zeta(t) = \zeta(t) - \zeta(t_o) = \sum_{n=0}^{N} \Delta\zeta^{(n)}(t) \qquad (26)$$

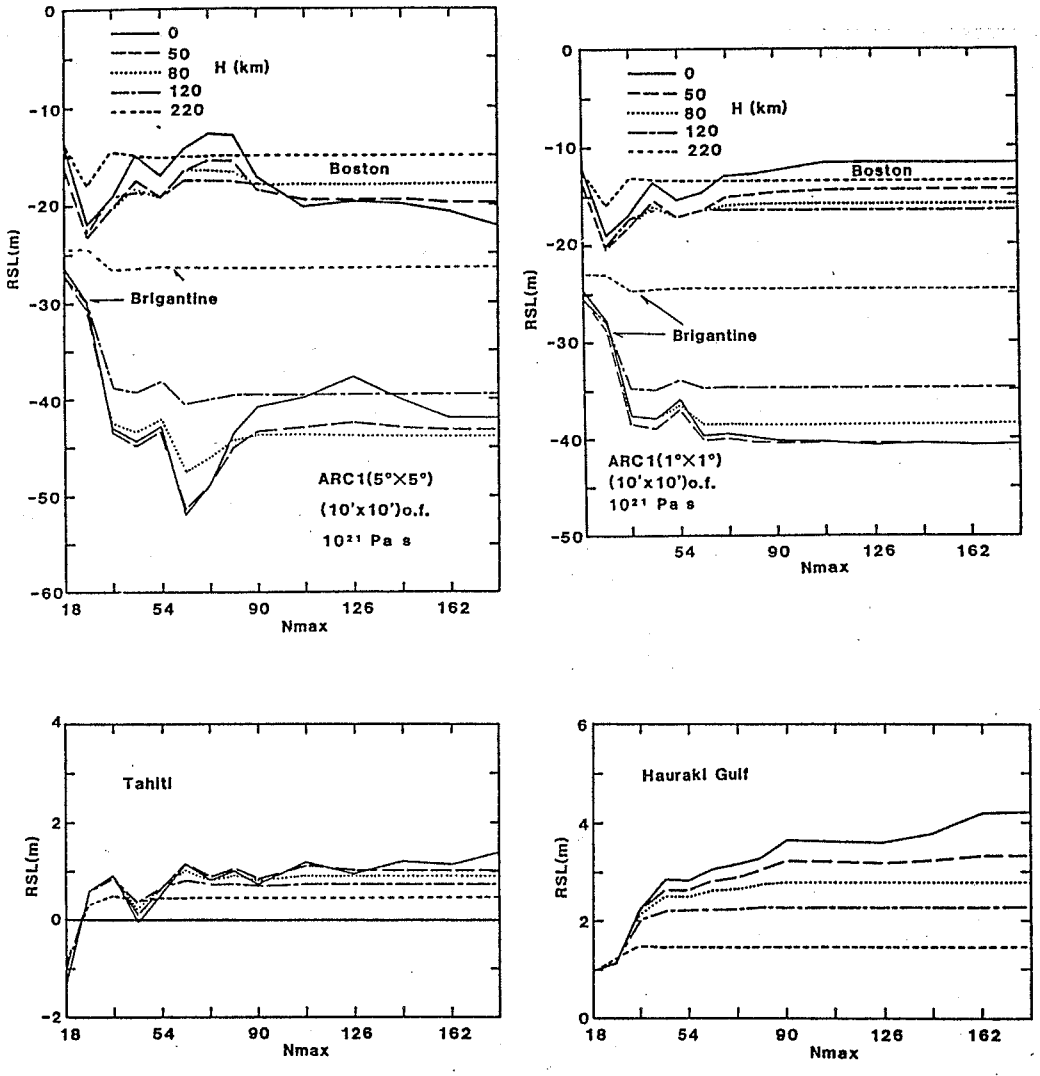

Figure 5: (a) Relative sea-level change $\Delta\zeta(t)$ as a function of N_{max} (equation 26) for a 5° resolution of the ice model at a site near the ice sheet margin.
(b) Same as (a) but for the 1° ice model.
(c) Same as (a) but for the far-field site of Tahiti.
(d) Same as (c) but for a site on the Hauraki Gulf of New Zealand.

Figure 5 illustrates $\Delta\zeta(t)$ for different degrees N_{max} of truncation of the expansion. In Figure 5 a comparison is also made at sites near the edge of the ice sheet for both the 5° and 1° descriptions of the the ice load. What these results indicate is that (i) convergence of the expansion can be very slow, particular for the coarse definition of the ice load, (ii) the value of $\Delta\zeta_i$ at convergence is not the same for the two loads because they define different mass distributions in the vicinity of the site, (iii) the convergence can be accelerated by introducing Earth models with thick lithospheres. Figures 5c and 5d illustrate the convergence at two sites far from the ice sheet and here the dominant factor is the description of the nearby water load. The island of Tahiti has a diameter of about 40 km and the meltwater load corresponds approximately to an infinite plate with a hole in it. If the resolution of the ocean function cannot resolve the island then the island moves up or down with the sea floor but if the island is resolved by the ocean function then some differential movement occurs as mantle material beneath the ocean is forced beneath the island. The maximum n required in the expansion is a function of lithospheric thickness and exceeds about 90 for H = 50 km. More extreme is the result for the Firth of Thames on the Hauraki Gulf of New Zealand, a shallow sea of about 100 by 150 km dimensions. In all examples the convergence is accelerated if the lithospheric thickness is increased but convergence is not on the same value in each instance.Because of the requirement of these very high, resolutions of the load, it may appear that a better approach than spherical harmonic expansions is to use a finite element formulation with a grid size that varies with distance from the point at which the sea-level response is to be evaluated. However when this response is evaluated globally for a large number of sites then the harmonic expansion solutions are the most convenient, provided that the convergence requirements are met. In the following solutions the ocean function is defined with a 10' resolution and expanded into spherical harmonics up to degree 180. The ice sheets are modelled with a 1° resolution and also expanded out to this maximum degree. For sites near the ice margin this is still not adequate but generally the detailed information required to evaluate the response at these sites with high accuracy is not available in any case.

5. CHARACTERISTICS OF THE THEORETICAL SEA-LEVEL CURVE

Equation (20) is solved for the three components $\zeta_r, \zeta_i, \zeta_w$ using ice models for the Arctic and Antarctic ice sheets. The Arctic model includes the Laurentide and Cordilleran ice domes and the Fennoscandian ice dome as defined by the ICE1 model of Peltier & Andrews (1976) but smoothed and defined with 1° resolution (the ARC1 model of Nakada and Lambeck 1987, 1989). The 1° resolution model ARC3 includes an ice sheet over the Barents and Kara Seas of the northwestern Soviet Union. The Antarctic model ANT3 is a maximum ice model discussed by Nakada & Lambeck (1987, 1989).

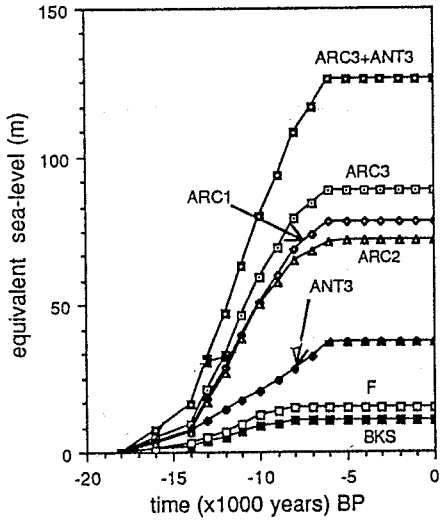

Figure 6: Equivalent sea-level curves for the Arctic ice models ARC1, ARC2, ARC3 and the Antarctic ice model ANT3. ARC1 is a 1° interpolated version of model ICE1 by Peltier and Andrews (1976). ARC2 corresponds to an interpolated version of ICE2 of Wu and Peltier (1983) which represent an adjustment of ICE1 to better fit the observational data. This model is therefore a function of the Earth model adopted by them. ARC3 is ARC1 plus a schematic model for the Barents-Kara ice sheet (BKS). All Arctic models include a Fennoscandian ice dome (F). AN3 is from Nakada and Lambeck, 1987, 1988).

The zero order approximation to the sea-level change resulting from the melting of these ice models is the time dependent equivalent sea-level curve (esl) defined by equations (1) and (9) and this function is illustrated in Figure 6. This curve can be approximately constrained by sea-level observations between 18 000 and 6000 years ago at far-field sites (Nakiboglu et al. 1983; Nakada and Lambeck 1988) and the adopted ice models are consistent with these observations. A number of different Earth models covering a range of plausible viscosity profiles are used and the appropriate parameters are discussed in Table 1. The mantle has been divided into two layers: an upper region, extending from the base of the lithosphere to the 650 km seismic discontinuity, and a lower mantle.

The solutions are expressed either relative to sea-level at the onset of glaciation, $\zeta(t)$ as defined by equation (23), or relative to the present level, $\Delta\zeta(t)$ as defined by equation (26). This latter quantity can also be expressed as the sum of 3 terms as

$$\Delta\zeta(t) = \Delta\zeta_r + \Delta\zeta_i + \Delta\zeta_w \qquad (27)$$

Table 1: Viscosity parameters for different Earth models used in forward modelling. All models use realistic elastic parameters and density profiles with the depth according to the model of Dziewonski and Anderson (1981).

Model	Viscosity (Pa s)	
	η_{um}	η_{lm}
E1	10^{20}	10^{21}
E2	$2x10^{20}$	10^{21}
E4	10^{21}	10^{21}
E14	$2x10^{20}$	10^{22}
E16	10^{21}	10^{22}
E28	10^{21}	10^{23}

where $\Delta\zeta_r$ defines the relative sea-level change on a rigid Earth, $\Delta\zeta_i$ in the additional contribution produced by the rebound of the crust as ice unloading proceeds, and $\Delta\zeta_w$ is the additional contribution produced by the deformation of the Earth in response to the water loading. Relative sea-levels have been predicted for a number of sites, including sites within the limits of the former ice sheets (Angerman River, Gulf of Bothnia, Northern Europe and Cape Henrietta Maria, Hudson Bay, Canada), in the near-field, near the margins of these ice sheets (e.g. Boston and the nearby sites of Barnstable, Massachusetts), in the intermediate field such as Bermuda or The Hague (Netherlands), and in the far-field in Australia and the South Pacific.

The rigid body term ζ_r. The rigid term ζ_r represents the effect of the rise or fall in sea-level resulting from deglaciation or glaciation on a rigid Earth with the requirement that the new sea surface remains an equipotential at all times. Within the ice sheet itself the shift of the equipotential surface is the sum of two opposing contributions: as melting proceeds the equipotential drops because of the reduced gravitational attraction of the ice load but at the same time it rises because the water level rises as melting proceeds. (Imagine the case of a vertical hole through the ice with a connection to the open sea. In reality the result has only sense from the time onwards when the site is exposed to the open sea.) At the Angerman River site in the Gulf of Bothnia, near the centre of the former Fennoscandian ice dome, the two parts contributing to ζ_r are almost equal but of opposite sign, with the result that ζ_r is nearly zero. For sites within the larger Laurentide ice sheet, the gravitational term exceeds the rise in sea-level term and the equipotential falls as melting proceeds (see results for Cape Henrietta Maria, Figure 7). Near the edge of the ice sheet the rise in water level exceeds the gravitational attraction of the ice and the net result is a rise in sea-level but at a rate that is less than the rate at which melt-water is added into the oceans. Further away from the ice sheet the rigid term is primarily one of a rise in sea-level from 18000 to about 6000 years ago as the melt water is added into the ocean. until it approximates the equivalent sea-level curve. Near the Hawaiian ridge, $\zeta_r \lesssim \zeta_{esl}$ but further south $\zeta_r \gtrsim \zeta_{esl}$.

The ice unloading term ζ_i. The term ζ_i is produced by the Earth's non-rigid response to the change in the ice load and it will be a function of the evolution of the ice load geometry with time as well as of the Earth's response function. At sites within the ice sheet the ζ_i term is one of an apparent lowering of sea-level as the crust emerges after unloading. At Cape Henrietta Maria, for example, ζ_i has a predicted amplitude of about 700 m for the ice-earth model ARC3-E4 (Figure 7a). The ice thickness at maximum glaciation was about 3000 m and the maximum rebound would be about 1200 m if a state of local isostasy had been achieved by the time the ice sheets reached their maximum extent. Observational estimates are not available of the maximum rebound that has occurred since the commencement of deglaciation, but observations at later times indicate that the rebound is less than predicted from the simple isostatic

models. This is a result of several factors; (i) of the lithosphere possessing a finite strength so that part of the load is supported by the flexural stresses within this layer and the isostatic compensation is regional rather than local, (ii) of regional isostasy not having been achieved at the time of onset of deglaciation, because of the mantle viscosity, and (iii) of the rebound not yet being complete.

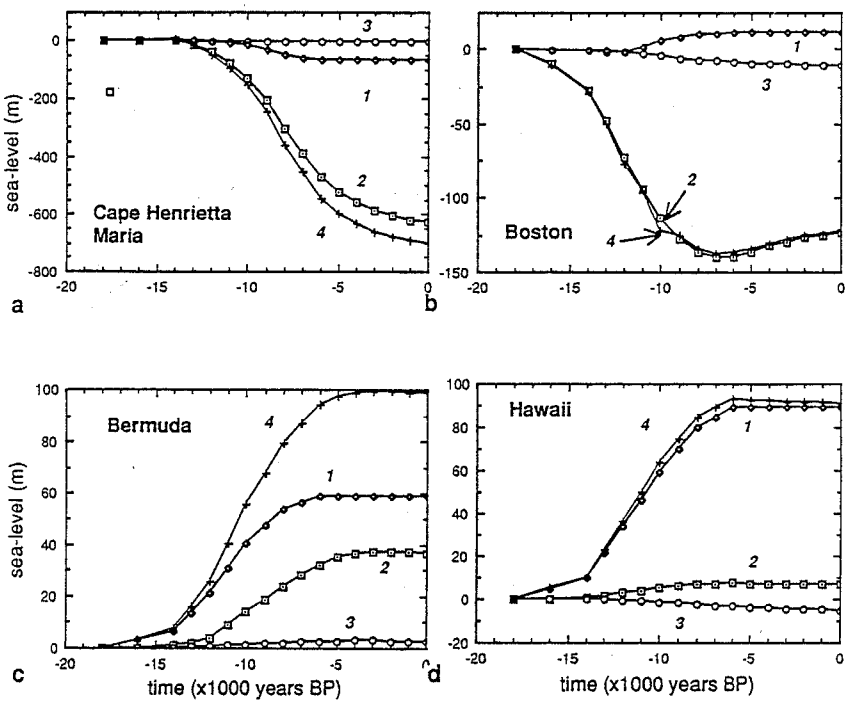

Figure 7: Predicted contributions to the sea-level change as defined by equation (20) at four different sites. Curve 1 corresponds to ζ_r, curve 2 to ζ_i, curve 3 to ζ_w and curve 4 to the total ζ. All change is with respect to sea-level at the onset of deglaciation at 1800 years ago.

Near the margins of the ice sheet the terms ζ_i and ζ_r are generally of opposite sign, ζ_r rises as melting proceeds whereas ζ_i falls, but ζ_i generally exceeds ζ_r in magnitude and the sea-level change from the combined effect is primarily one of an apparent falling level (Figure 7b). The ice unloading term here is spatially variable over quite short distances in the vicinity of the former ice margins and the predictions are about equally sensitive to mantle rheology and ice model parameters. Further from the ice front, at sites free from past localized ice loading, the two terms are of comparable magnitude

(Figure 7c) although at some sites the sign of ζ_i changes with time: initially the predicted ζ_i is an apparent fall in sea-level as the crust rebound to the early stage of unloading but later, as the ice retreats further from the site, an apparent rise in sea-level is predicted and this amplifies the ζ_r term.

The water loading term ζ_w. Compared to ζ_r and ζ_i the melt-water term ζ_w is small in the near-field (Figure 7), rarely exceeding 20 m for the combined ARC3 and ANT3 ice models. In the far-field after termination of deglaciation, ζ_w is generally larger than ζ_i (Figure 8). In a first approximation the time dependence of the ζ_w term is proportional to $(\zeta_r + \zeta_i)$ and at sites far from the ice sheet this dependence follows closely the equivalent sea-level curve. The amplitude of ζ_w is a function of the load distribution in the vicinity of the site and is therefore a function of the coastal geometry as well as of $(\zeta_r + \zeta_i)$ and the term may vary spatially over even relatively short distance if the coastline geometry is complex (Figure 8). In contrast ζ_i remains relatively constant over a given area of the far-field. Differential values of the sea-level between nearby sites n,m far from the ice sheets,

$$\delta\zeta_{nm} = \Delta\zeta_n - \Delta\zeta_m, \tag{28a}$$

are largely independent of the other two contributions and reflect primarily the response of the mantle beneath the sites to the change in water load through time, or

$$\delta\zeta_{nm} \cong \Delta\zeta_{w(n)} - \Delta\zeta_{w(m)}. \tag{28b}$$

Relative sea-level curves. The relative sea-level, as defined by (26) is the sum of the three terms $\Delta\zeta_r$, $\Delta\zeta_i$, $\Delta\zeta_w$ each of which varies spatially and temporally in a complex manner. The relative sea-levels are likewise predicted to exhibit considerable variability and no single curve adequately characterizes the sea-level change. Predicted sea-levels are a function of both the ice and earth-response parameters but, as illustrated by the above examples, this dependence varies with geographical location and time. This means that by comparing model predictions with observations of sea-level change it does become possible to separate these parameters. Figures 9-14 illustrate a range of predictions for sea-level change as a function of mantle viscosity, lithospheric thickness, and ice models which demonstrate that the separation of parameters can be achieved if adequate observational data can be found. For the period up to about 6000 years ago, the relative sea-level change in the far-field is insensitive to mantle parameters within a broad range of viscosities, lithospheric thickness, and details in ice loads. It is, however, strongly dependent on the equivalent sea-level rise; on the rates and timing of the melt-water addition (Figure 9). Particularly important is the sea-level at the time of onset of deglaciation as this constrains the total volume of melt-water. Far-field observations of sea-level, therefore, constrain the gross aspects of the Arctic and Antarctic ice models.

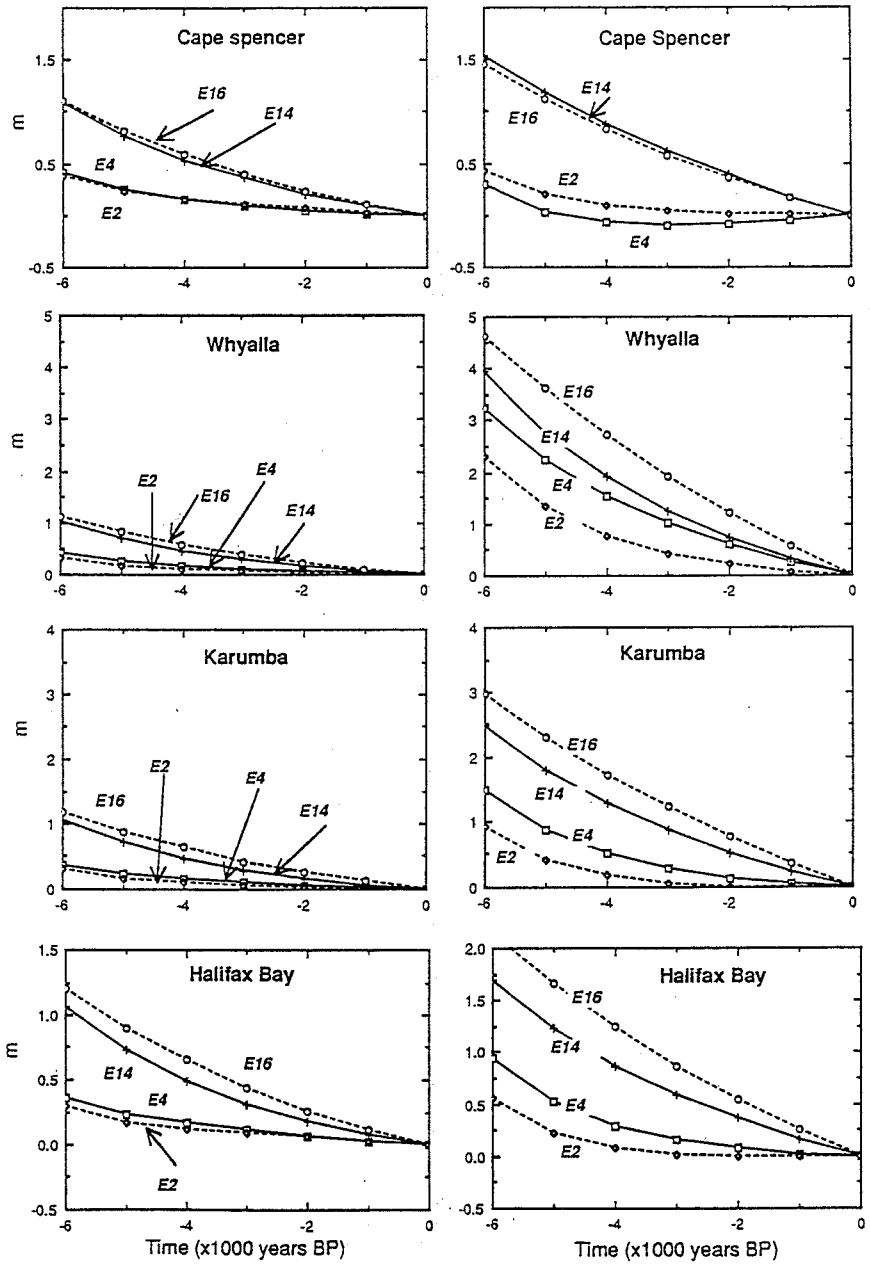

Figure 8: Contributions to relative sea-level at far-field sites during the Late Holocene. The $\Delta\zeta_i$ terms are given on the left and the $\Delta\zeta_w$ terms are given on the right for four Earth models (Table 1). (Note different scales used.) Whyalla and Cape Spencer are two sites about 300 km apart in the Spencer Gulf of South Australia and Karumba and Halifax Bay lie about 600 km apart on opposite sides of the Cape York Peninsula of Northern Queensland. Differential values of sea-level between nearby sites n,m far from the ice sheet

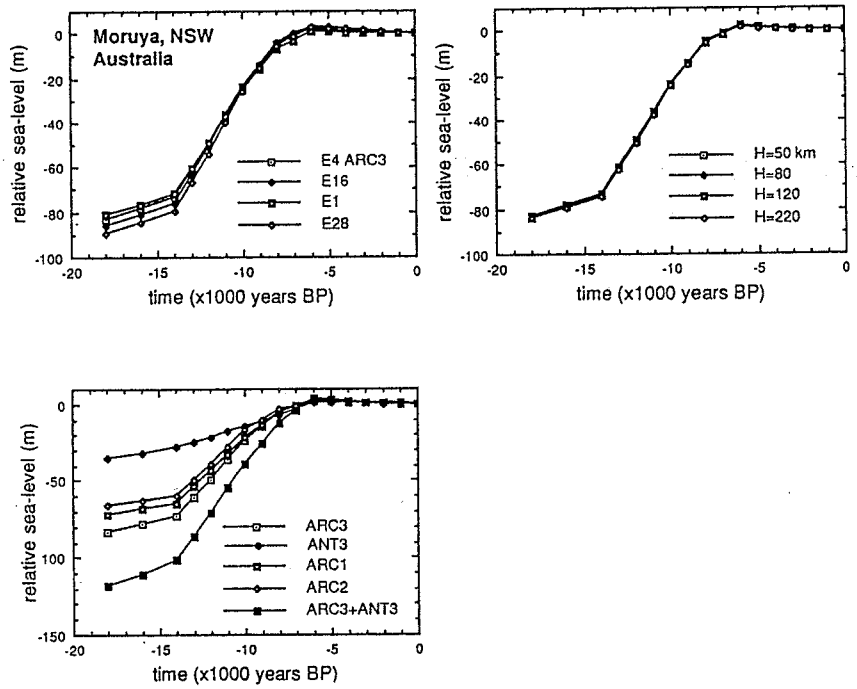

Figure 9: Predicted sea-level change for past 18000 years at the far-field site of Moruya (New South Wales, Australia) as a function of mantle viscosity, lithospheric thickness and ice model.

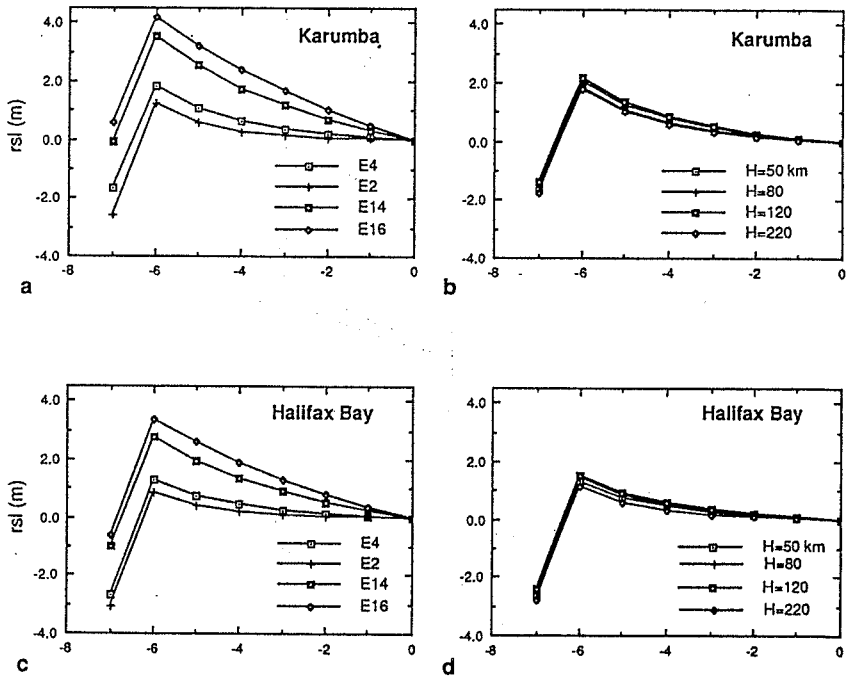

Figure 10: Predicted sea-levels at two far-field continental margin sites for past 7000 years.

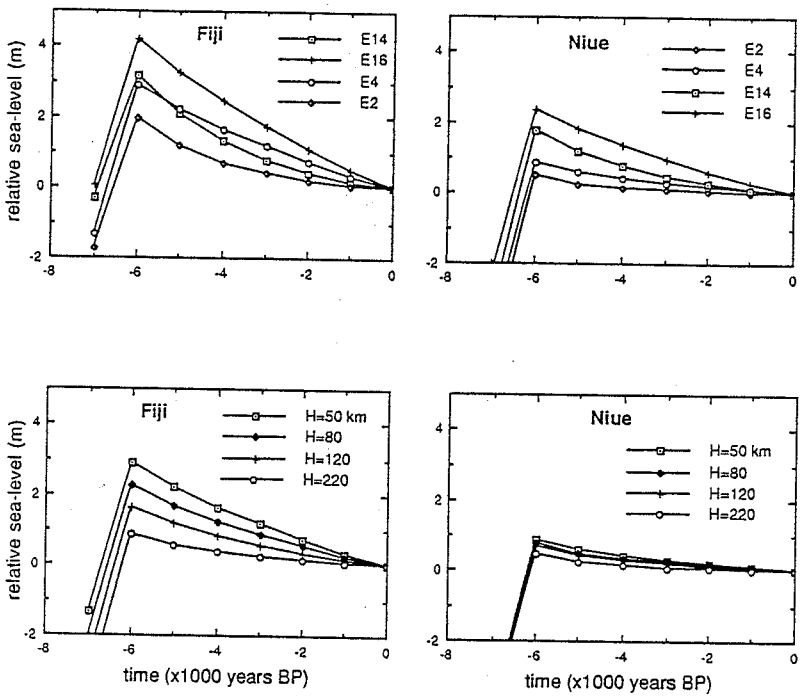

Figure 11: Same as Figure 10 but for island sites. The Fiji island of Viti Levu has a diameter of about 130 km compared with about 20 km for Niue.

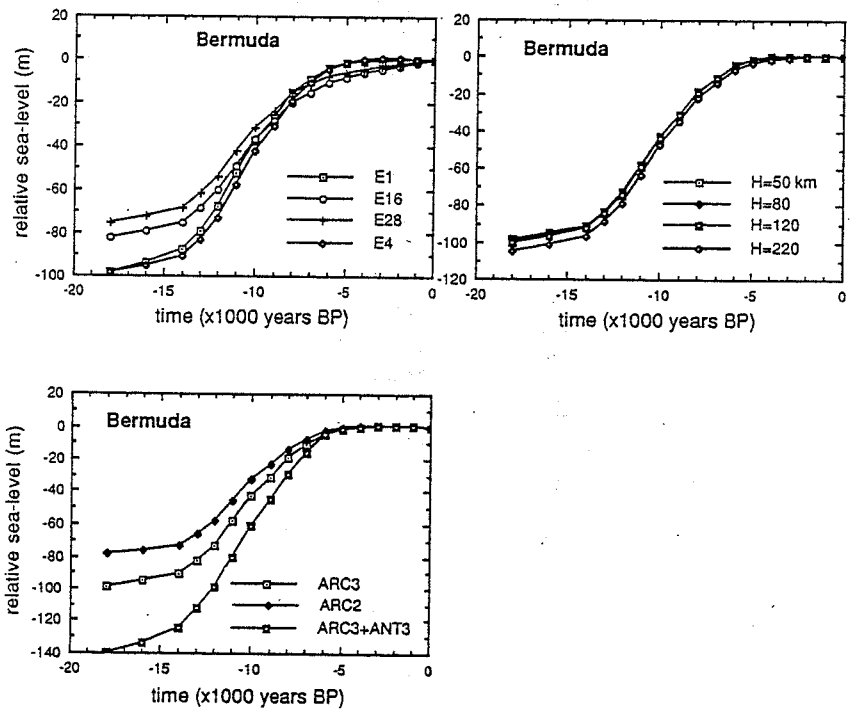

Figure 12: Same as Figure 9 but for a site in the intermediate field.

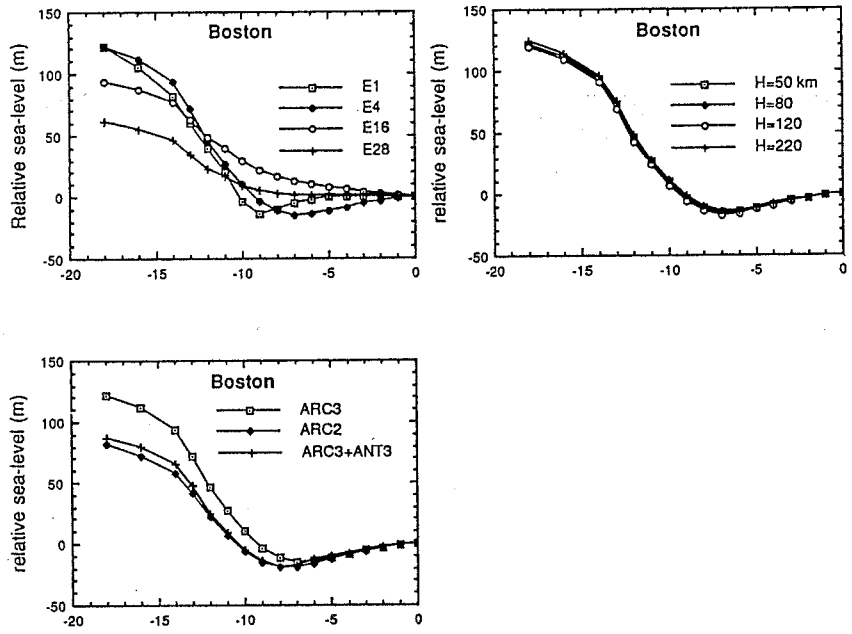

Figure 13: Same as Figure 9 but for a site near the ice margin.

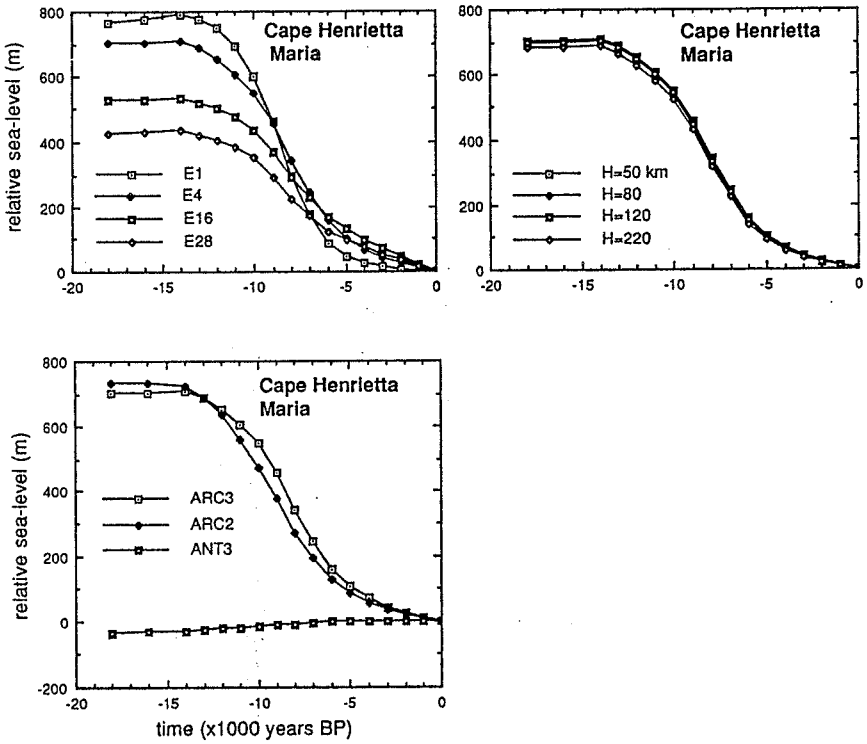

Figure 14: Same as Figure 13 but for a site near the centre of the Laurentide ice sheet (Cape Henrietta Maria).

The predicted far-field sea-levels along continental margins for the past 7000 years are characterized by a maximum value of up to a few metres above the present value at about 6000 years ago. A careful examination illustrates considerable regional variations in these amplitudes because of the melt-water term $\Delta\zeta_w$ which is strongly dependent on coastal geometry. This is illustrated in Figure 10. Here, spatial differential values, as defined by equation (28) provide a sensitive measure of Earth structure, largely free from assumptions made about the ice models (Nakada and Lambeck 1989). The absolute values of these highstands provide a means of fine-tuning the ice melting models in the past 6,000 years, once the Earth structure is established from the differential values. An important point is that these far-field spatial differential values are primarily sensitive to mantle structure near the sites, and not to global structure. This opens, therefore, the possibility of examining lateral variations in mantle viscosity. Important here are observations from ocean islands because predictions for nearby islands of different sizes indicate that differences in sea-levels are good indicators of mantle structure (Figure 11).

At sites in the intermediate field, such as Bermuda (Figure 12) the sea-level change is a function of both the rigid and ice terms and for the past 6000 years the ice term $\Delta\zeta_i$ remains important. For models of relatively low viscosity (e.g. E1 and E4) the sea-levels are predicted to have reached their present value already several thousand years ago whereas for higher viscosities (e.g. models E16 or E28) sea-level will still be encroaching on the island (i.e. the island is subsiding).

Close to the ice margins the predicted sea-levels vary rapidly with positions relative to the ice front at the time of glaciation and major differences occur between nearby sites. The observations are particularly dependent on the assumed ice model (Figure 13) but also on mantle viscosity. Spatial differential values (equation 28) of sea-level may be useful here in separating out the two factors. Predictions for nearby sites, for example, are approximately independent of mantle viscosity unless the upper mantle value is $\gtrsim 5\text{x}10^{20}$ Pa s and the lower mantle value is 10^{21} Pa s. Likewise, the differential values are approximately independent of lithospheric thickness unless this value is $\gtrsim 200$ km. However, because the available number of observations are usually small and the number of parameters required to model the ice sheet is large, it will generally not be possible to invert the differential observations to obtain unique ice models (Quinlan, 1981). For example, the ARC2 ice model has the same effect on sea-level at Boston as does the addition of the Antarctic ice sheet.

Within the limits of the former ice sheet margin $\zeta_i >> \zeta_r, \zeta_w$ and the relative sea-level curve is determined almost wholly by the response of the crust to the unloading of the surrounding ice sheet. Here the predicted rebound is relatively insensitive to the details of the ice models at the margins but it is sensitive to the thickness of the ice sheet (Figure 14). The horizontal dimensions of the Fennoscandian ice sheet are of the order

of 1000-1500 km and the rebound is primarily sensitive to upper mantle viscosity. The rebound due to the much larger Laurentide ice sheet is, however, sensitive to the viscosity structure of the entire mantle.

6. PRINCIPAL CONCLUSIONS AND UNRESOLVED QUESTIONS

The predictions discussed in the preceding section and illustrated in Figures 9-14 do indicate that the sea-level change associated with the late Pleistocene melting can be expected to exhibit a complex global pattern. Observations from a variety of regions are generally consistent with this variability. In order to predict this change globally and with accuracy, it is necessary to have a detailed knowledge of the melting histories of the ice sheets, both spatially and temporally. Adequate information is generally not available from glaciological information alone. There remains, for example, debate about the volume of ice locked up in the ice sheets and about the extent of these ice sheets in the northern hemisphere. Estimates of the Late Pleistocene ice sheet over the continental shelf of the Barents and Kara Seas (north-western Soviet Union) range from nearly zero to a volume equal to the Fennoscandia ice sheet. Eastern Siberia has generally been assumed to have been free from major ice domes during the last glacial but recently it has been suggested that a Pleistocene ice sheet existed here that rivalled the Antarctic ice sheet. There remains a similar uncertainty about the extent of Late Pleistocene melting of the Antarctic ice sheet.

The examination of past sea levels can contribute significantly to establishing constraints on these ice volumes and on locating the centres of loading. For example, observations of sea-level in the far-field generally indicate that this level was 130-150 m below the present level (e.g. Chappell, 1987). The predictions of these levels at the far-field sites are not strongly dependent on mantle rheology and they approximate closely the equivalent sea-level estimate. This is not so for sites closer to the ice sheet such as Bermuda and Florida and observations from sites in the intermediate field may not be a reliable indicator of equivalent sea-level, and their use could lead to a systematic underestimation of past ice volumes.

The examination of sea-level change near the postulated ice domes can also provide an important way of testing these glacial hypotheses. Raised beaches in the vicinity of the Antarctic base Davis, for example, establish that rebound has occurred in Holocene time and this points to unloading of the Antarctic ice sheet. From a single site the volume of unloading cannot be established and further examination of the Antarctic shoreline and far southern islands is necessary. Similarly, a re-examination of the Eurasian Arctic shorelines may be rewarding.

The far-field observations of sea-level from 12000-6000 years ago establish the equivalent sea-level curve for the latter part of the last deglaciation cycle. A possible

problem here, however, concerns the time scale. Ice models are constrained largely by radiocarbon dates but varve chronologies have also been used and the two may differ significantly. The sea-level data is constrained mainly by radiocarbon ages, but sometimes uranium-thorium dates are used. If radio-carbon ages are used for both ice and sea-level data the time scale is consistent but not necessarily uniform. Even the consistency can be challenged because generally the major corrections for fractionation and reservoir effects are not made and these can be significant if the dated materials represent different environments (marine or estuarine water, submarine or subaereal). Lambeck and Nakada (1989) discuss this problem further in the context of the northwestern European sea-level and rebound evidence. Within the limitations of this time scale question, the far-field sea-level observations indicate that substantial melting of Antarctic ice occurred in phase with, or possibly as much as 1000 years after, the Laurentide melting (Nakada and Lambeck, 1988b). If this can be substantiated, this presents evidence on how the Antarctic ice sheet responds to rising sea-level, an important question in evaluating possible future sea-level change.

The predictions for the past sea-levels in the far-field exhibit considerable variability in amplitude and timing of the occurrence of the highstand at about 6000 years ago. The amplitudes are small, ranging from a few tens of centimetres to a few metres, but the precision of the observations is also high (e.g. Chappell et al. 1982). The regional variation in these amplitudes provide important constraints in mantle structure (Nakada and Lambeck, 1989). Preliminary analyses suggest that the upper mantle has a viscosity that may be 50 times less than the lower mantle, and that regional variations in upper mantle viscosity occur, with continental mantle having a higher viscosity than oceanic mantle.

An important aspect of these predictions is that they indicate that very high resolution models are essential. Coastline geometry must be modelled with very high resolution and, in many localities, it is necessary to model the time dependence of the coastline as sea-level rose during Holocene time if the highstands are to be modelled with precision. High accuracy models of the ice sheet melting are also essential if sea-levels are modelled near the ice sheet margins. This information is generally not available and sea-level observations from near the ice margin are of limited value for modelling the Earth's response.

Another unresolved question concerns the assumption of the linear viscoelastic response for the Earth. Perhaps the only justification for this choice is that it is mathematically convenient. It means that the viscosity parameters should be considered as effective parameters only and their interpretation in terms of realistic physical parameters requires caution. However, no observational evidence at this stage warrants the introduction of a non-linear rheology for modelling glacial rebound, particularly at

site far from the centres of ice unloading. Other modelling questions concern the question of whether the mantle is treated as adiabatic or non-adiabatic (Cathles, 1975; Fjeldskaar and Cathles, 1984). A further question concerns the effect of earlier cycles of glaciation and deglaciation (Wu and Peltier, 1983; Nakada and Lambeck, 1987). Clearly much work remains to be done before we can conclude that the glacial rebound problem is solved but the progress made over the past decade or so, and the importance of the goals that can be achieved, make further study worthwhile.

REFERENCES

Budd WF, Smith IN (1987) Conditions for growth and retreat of the Laurentide ice sheet. Geography. Phys. Quat. 41: 312-321.

Budd WF, Smith IN (1981) The growth and retreat of ice sheets in response to orbital radiation changes. In Sea Level, Ice and Climatic Change. Int. Asst. Hydrol. Sci. Publ 131: 369-409.

Cathles LM (1975) The Viscosity of the Earth's Mantle. Princeton University Press, New Jersey.

Chappell J (1987) Late Quaternary sea-level changes in the Australian region, in Sea-level Changes: 296-331, eds. Tooley MJ, Shennan I, Basil Blackwell, New York.

Chappell J, Shackleton, NJ (1986) Oxygen isotopes and sea-level. Nature 324: 137-140.

Chappell J, Rhodes EG, Thom BG, Wallensky EP (1982) Hydro-isotasy and the sea-level isobase of 5500 B.P. in north Queensland, Australia. Mar. Geol. 49: 81-90.

Dziewonski AM, Anderson DL (1981) Preliminary reference Earth model. Phys. Earth planet Int. 25: 297-356.

Farrell WE, Clark JA (1976) On postglacial sea-level. Geophys. J.R. astr. Soc. 46: 647-667.

Fjeldskaar W, Cathles LM (1984) Measurement requirements for glacial uplift detection of nondiabatic density gradients in the mantle. J. Geophys. Res. 89: 10115-10124.

Hughes TJ (1981) Numerical reconstruction of paleo-ice sheets in Denton & Hughes (1981): 222-261.

Lambeck K (1988) Geophysical Geodesy: The Slow Deformation of the Earth. Oxford University Press, 718 pp.

Lambeck (1989) Glacial rebound, sea-level change, and mantle viscosity (1989) Harold Jeffreys Lecture. Q.J. Roy. Astron. Soc. (in press).

Lambeck K, Nakaka M (1989) Glacial rebound and sea-level change in Northwestern Europe. Geophys. J. (subm.).

McConnell, RK (1968) Viscosity of the mantle from relaxation time spectra of isostatic adjustment. J. Geophys. Res. 73: 7089-105.

Nakada M, Lambeck K (1987) Glacial rebound and relative sea-level variations: a new appraisal. Geophys. J. R. astr. Soc. 90: 171-224.

Nakada M, Lambeck K (1988) The melting history of the late Pleistocene Antarctic ice sheet. Nature 333: 36-40.

Nakada M, Lambeck K (1989) Late Pleistocene and Holocene sea-level change in the Australian region and mantle rheology. Geophys. J. 96: 497-517.

Nakiboglu SM, Lambeck K, Aharon P (1983) Postglacial sea-levels in the Pacific: implications with respect to deglaciation regime and local tectonics. Tectonophys. 91: 335-358.

Paterson WSB (1972) The Physics of Glaciers. Pergamon, New York.

Peltier WR (1974) The impulse response of a Maxwell Earth. Res. Geophys. Space Phys. 12: 649-69.

Peltier WR, Andrews JT (1976) Glacial isostatic adjustment-I: The forward problem. Geophys. J.R. astr. Soc. 46: 605-46.

Quinlan GM (1981) Numerical models of postglacial relative sea-level change in Atlantic Canada and the Eastern Canadian Arctic. Thest, Dalhousie University Halifax.

Walcott RI (1972) Late Quaternary vertical movements in eastern North America. Rev. Geophys. 10: 849-884.

Wu P, Peltier WR (1983) Glacial isostatic adjustment and the free air gravity anomaly as a constraint on deep mantle viscosity. Geophys. J.R. Ast. Soc. 74: 377-449.